

MONOCYCLE SHAPES FOR ULTRA WIDEBAND SYSTEM

Xiaomin Chen

Dept. of Electrical Engineering
Arizona State University
Campus Box 875706
Tempe, AZ 85287-5706

Sayfe Kiaei

Dept. of Electrical Engineering
Arizona State University
Campus Box 875706
Tempe, AZ 85287-5706

ABSTRACT

Ultra Wideband (UWB) is a promising technique for wireless communications. It is a carrier-free (base-band) technique, which will greatly reduce the complexity and cost of the transceiver. In contrast with the conventional communication systems using the "sine wave", UWB information is carried in very short pulse, which covers an extremely wide spectrum bandwidth. In this paper, several candidate monocycle shapes are investigated, their spectrum characteristics and BER performance in AWGN using pulse position modulation (PPM) are simulated and the results are compared. Their performances in fading multipath channel are also investigated.

1. INTRODUCTION

UWB is a newly developed wireless RF technology, and is considered to be a potential solution to a wide range of RF problems. UWB transmitters transmit trains of extremely short pulses at precise time intervals, resulting in a very low power, noise-like signal that can coexist with other radio systems. Its features can be summarized as [3]:

- Ultra wideband and ultra-low PSD
- Base-band communications
- Excellent immunity to interference from other radio systems
- Excellent multipath immunity
- Low probability to intercept and detect

In UWB communications, information is contained in narrow pulses (monocycles), so the RF and analog circuitry is reduced to a wide band low-noise amplifier, a correlator and data converters. No up/down conversion or mixer is needed, which will result in substantial reduction of transceiver area, power, and can be integrated with low price CMOS circuit. A comparison of a direct IF sampling transceiver and a UWB transceiver architecture is shown in Figure 1 and Figure 2. It illustrates that the UWB transceiver could be implemented as a simple integrated circuit chipset with very few off-chip components.

The UWB signaling emitted by the k^{th} transmitter using pulse position modulation can be represented by [2]

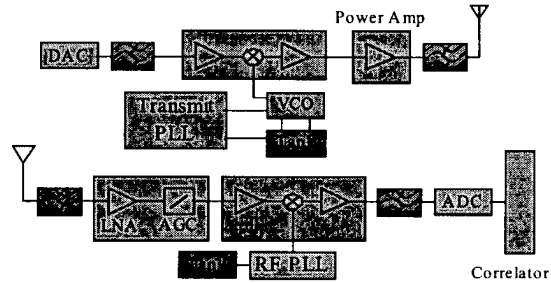


Figure 1. Direct IF sampling transceiver architecture

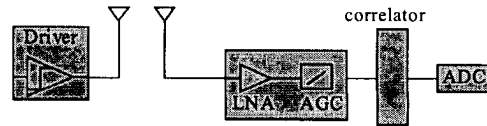


Figure 2. UWB transceiver architecture

$$s_r^{(k)}(t^{(k)}) = \sum_j w_r(t^{(k)} - jT_f - c_j^{(k)}T_c - \delta \cdot d_{\lfloor j/N_s \rfloor}^{(k)}) \quad (1)$$

Here $w_r(t)$ is the transmitted monocycle waveform and T_f is the pulse repetition time and is generally much larger than the monocycle width. $\delta \cdot d_{\lfloor j/N_s \rfloor}^{(k)}$ represents the data modulation. Each link is assigned a distinct, pseudorandom time hopping code $\{c_j^{(k)}\}$ and $c_j^{(k)}T_c$ defines a pseudorandom additional time shift to the j^{th} monocycle.

At the receiver, when N_u links are active, then the received signal can be represented by [2]

$$r(t) = \sum_{k=1}^{N_u} A_k s_{rec}^{(k)}(t - \tau_k) + n(t) \quad (2)$$

Here A_k models the attenuation of the k^{th} transmitter signal and τ_k represents time asynchronism between the clocks of the k^{th} transmitter and the receiver.

In AWGN, the optimum receiver for a single bit of a binary UWB signal is reduced to a correlator:

"decide $d_0^{(1)}=0$ " \Leftrightarrow

$$\sum_{j=0}^{N_s-1} \int_{\tau_1+jT_f}^{\tau_1+(j+1)T_f} r(t)v(t-\tau_1-jT_f-c_j^{(1)}T_c)dt > 0 \quad (3)$$

where $v(t)=w_{rec}(t)-w_{rec}(t-\delta)$ is the correlation template. In a multi-user environment, it is reasonable to approximate the combined effect of the other users' dehopped interfering signals as a Gaussian random process, and thus the same reception algorithm can be used [2].

2. MONOCYCLE SHAPES FOR UWB

UWB is a base-band technology, and thus the choice of the monocycle shape will affect the performance. Several possible monocycles (duration = 0.5 ns) for UWB are listed below and their comparison will be illustrated in section 3.

2.1. Gaussian pulse

The Gaussian pulse can be represented by

$$w(t) = Ae^{-[(t-T_c)/T_{au}]^2} \quad (4)$$

where A is the amplitude and T_{au} is the pulse shape parameter. Its waveform and PSD are shown in Figure 3.

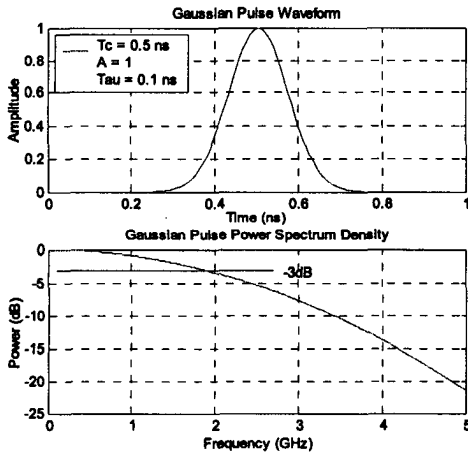


Figure 3. Waveform and PSD of Gaussian pulse

2.2. Gaussian monocycle

The Gaussian monocycle is similar to the first derivative of the Gaussian pulse and is given by [3]

$$w(t) = 2 \times \frac{A}{T_{au}} \times \sqrt{e} \times (t - T_c) \times e^{-2 \times [(t - T_c) / T_{au}]^2} \quad (5)$$

Its waveform and power spectrum density are illustrated in Figure 4.

2.3. Scholtz's monocycle

This monocycle appears in Dr. Scholtz's papers, so we call it Scholtz's monocycle. It is similar to the second

derivative of the Gaussian pulse and can be represented by [5]

$$w(t) = A \left[1 - 4\pi \left(\frac{t - T_c}{T_{au}} \right)^2 \right] \exp \left[-2\pi \left(\frac{t - T_c}{T_{au}} \right)^2 \right] \quad (6)$$

Its waveform and PSD is shown in Figure 5.

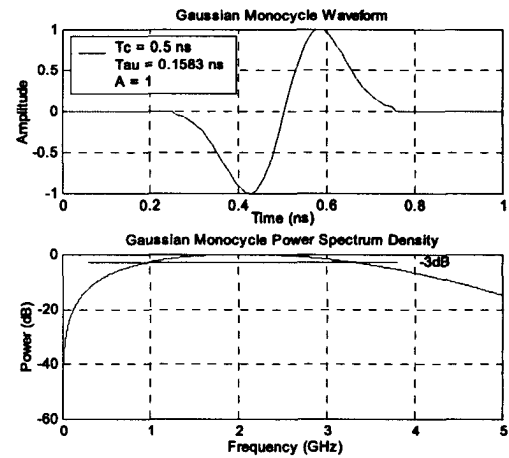


Figure 4. Waveform and PSD of Gaussian monocycle

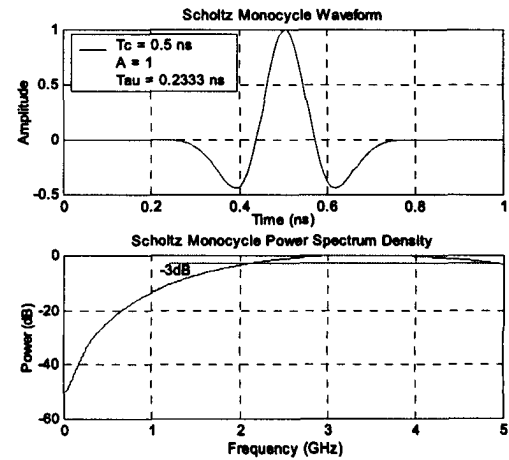


Figure 5. Waveform and PSD of Scholtz's monocycle

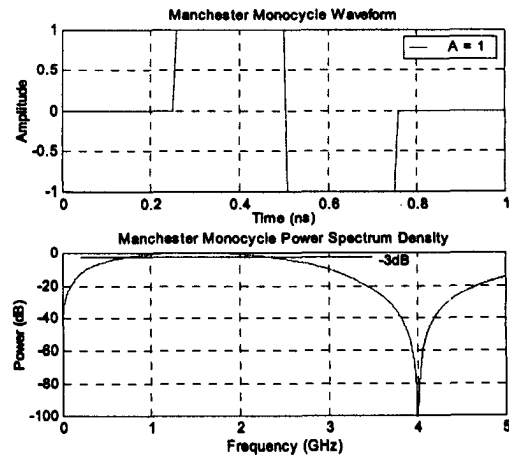


Figure 6. Waveform and PSD of Manchester monocycle

2.4. Manchester Monocycle

The Manchester monocycle has amplitude A during half of the monocycle width and has amplitude $-A$ during the other half. The waveform and PSD is shown in Figure 6.

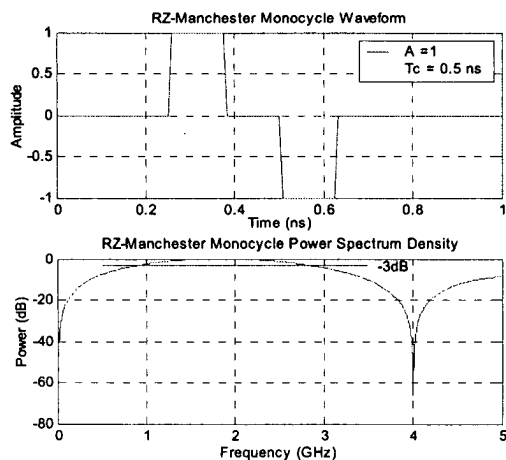


Figure 7. Waveform and PSD of RZ-Manchester

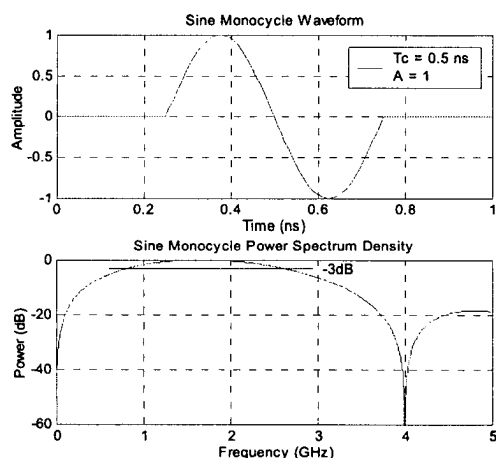


Figure 8. Waveform and PSD of sine monocycle

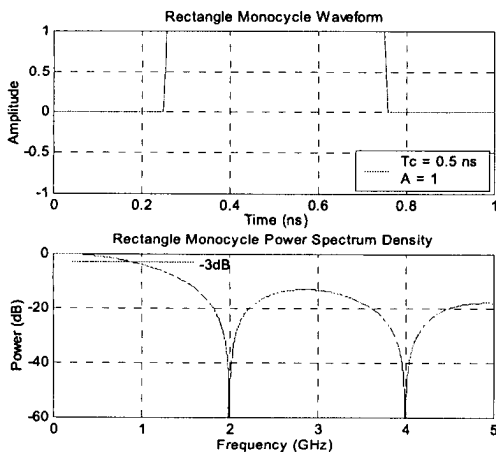


Figure 9. The waveform and PSD of rectangle monocycle

2.5. RZ-Manchester Monocycle

The return-to-zero Manchester monocycle has amplitude A and $-A$ for only a portion of each half monocycle width. The waveform and PSD is shown in Figure 7.

2.6. Sine Monocycle

The sine monocycle is simply just one period of a sine wave. The waveform and PSD is shown in Figure 8.

2.7. Rectangle Monocycle

The rectangle monocycle is a pulse that has uniform amplitude A during the whole pulse width. Its waveform and PSD is shown in Figure 9.

3. SIMULATIONS AND COMPARISONS

The objective of studying different monocycle shapes for UWB is to help to investigate the effect of the monocycle shapes on the design of filters, the choice of receiver bandwidth, the antenna design, the bit error rate performance and multipath performance. Thus, the spectrum characteristics of these monocycles are compared and their bit error rate performances in AWGN channel are simulated.

The spectrum characteristics for these monocycles are illustrated in section 2. In the bit error rate simulations described below, every monocycle width is chosen to be 0.5 ns, the ratio of T_f and T_m is set to be 1024 and T_{au} is chosen to make sure that the pulse amplitude is close to zero at the edge of the monocycle. The values of the T_{au} are also shown in the figures in section 2.

3.1 Monocycle Spectrum Characteristics

Unlike the conventional narrow-band communication systems, it is desirable for UWB signaling to spread the energy as widely in frequency (and hence the potential for interference to other systems). As shown in figures 3 - 9, Gaussian pulse and rectangle monocycle have dc components, which may reduce the antenna radiating efficiency. Scholtz's monocycle, Gaussian monocycle and RZ-Manchester monocycles have wider 3db bandwidth than others.

3.2 Single link BER performances in AWGN channel

As discussed in section 1, the optimum receiver in AWGN is a correlation receiver. Eq. (3) shows that the modulation parameter δ will affect the BER. The optimal choice of δ for a given received monocycle on a single link is given by [1]

$$\delta_{opt} = \arg \min_{\delta} \int_{-\infty}^{\infty} w_{rec}(t) w_{rec}(t - \delta) dt \quad (7)$$

Here $0 \leq \delta \leq T_m$, where T_m is the monocycle duration. Note that when δ is greater than T_m , $w_{rec}(t)$ and $w_{rec}(t-\delta)$ are orthogonal. Therefore δ_{opt} can be chosen as T_m . In our simulations, δ_{opt} for Gaussian pulse, Gaussian monocycle, Scholtz's monocycle, Manchester monocycle, RZ-Manchester monocycle, sine monocycle and rectangle monocycle are first determined by using Eq. (7). In this case, they are 0.5ns, 0.1917ns, 0.125ns, 0.25ns, 0.25ns, 0.25ns and 0.5ns respectively. The single-link simulation result is illustrated in Figure 10. It shows that the performances of Scholtz's, Manchester, RZ-Manchester, sine and Gaussian monocycle are better than those of Gaussian pulse and rectangle monocycle.

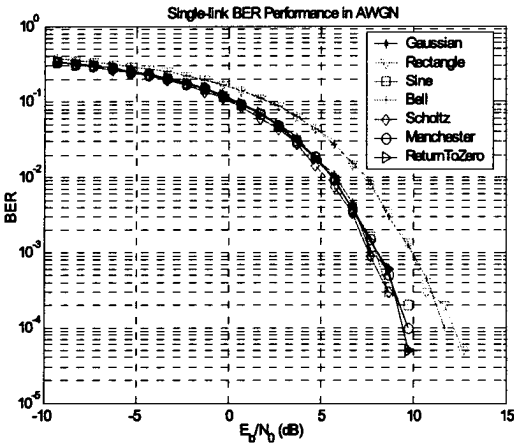


Figure 10. Single-link BER performance in AWGN channel

3.3 Multiple access BER performances in AWGN channel

As described in section 2, when multiple users are active, the same correlation receiver can be used. The BER performance with the number of users is shown in Figure 11. It shows that multiple access performances of Scholtz's monocycle, RZ-Manchester monocycle, Gaussian monocycle and Manchester monocycle are better.

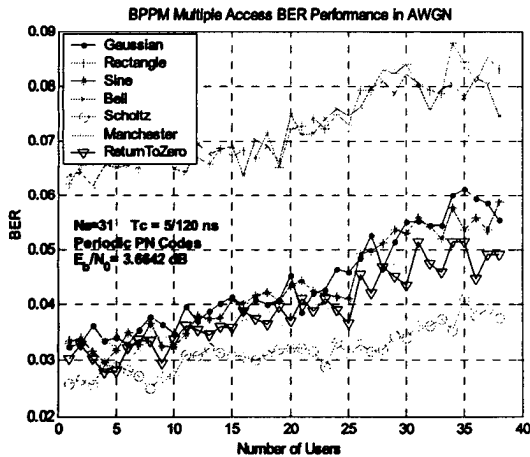


Figure 11. Multi-access BER performance in AWGN channel

3.4 Multipath BER performance in AWGN channel

There is no decent multipath model available for UWB today. In this simulation, deterministic two-path model are adopted [6]. The indirect path gain is chosen as -0.7 . Simulation results of bell and Scholtz's monocycle are shown in Figure 12. It shows that both the monocycle shape and the path difference affect the multipath performance.

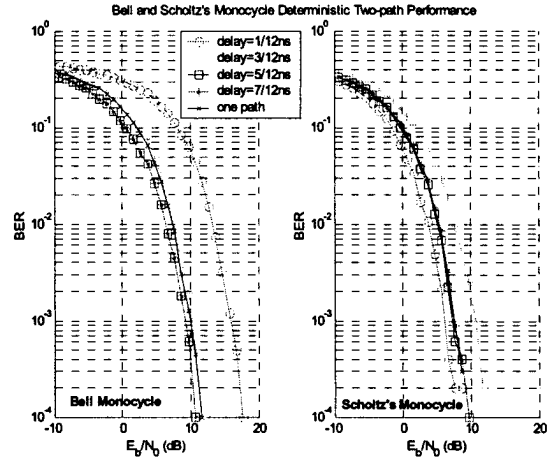


Figure 12. Deterministic two-path performance in AWGN channel

4. CONCLUSION

In this paper, several candidate monocycle shapes for UWB are described. Their single-link and multi-access performances are simulated and compared. Multipath performances of these monocycle shapes are also considered. The results show that monocycle shape affects the PPM BER and multipath performances. The monocycle shape also determines the spectrum characteristics of UWB signals. Based on these results, issues such as the design of wideband antenna, the effect of receiver bandwidth and tradeoffs between performance and implementation complexity can be further studied.

5. REFERENCES

- [1] R. A. Scholtz, "Multiple Access with Time-Hopping Impulse Modulation," *Proc. MILCOM*, Oct. 11-14, 1993
- [2] M. Z. Win and R. A. Scholtz, "Impulse Radio: How It Works," *IEEE Communications Letters*, vol.2, no.2, pp.10-12, Jan. 1998
- [3] Paul Withington, "Impulse Radio Overview", Time Domain Corp.
- [4] R. J-M. Cramer, M. Z. Win and R. A. Scholtz, "Impulse Radio Multipath Characteristics and Diversity Reception," *Proceedings of the 1998 IEEE International Conference on Communications, ICC'98*, vol.3, pp.1650-1654
- [5] Hojoon Lee, Byungchil Han, Yoan shin and Sungbin Im, "Multipath Characteristics of Impulse Radio Channels," *Conference Proceedings of the IEEE VTC-2000*, Tokyo, vol. 3, pp. 2487-2491, 2000.